J. Plasma Phys. (2017), *vol.* 83, 705830401
doi:10.1017/S0022377817000502

Variety of shapes of solar wind ion flux spectra: Spektr-R measurements

Maria Riazantseva[1,†], V. Budaev[1,2], L. Rakhmanova[1], G. Zastenker[1], Yu. Yermolaev[1], I. Lodkina[1], J. Šafránková[3], Z. Němeček[3] and L. Přech[3]

[1]Space Research Institute of the Russian Academy of Sciences (IKI), 117997 Moscow, Russia

[2]National Research Center 'Kurchatov Institute', 123182 Moscow, Russia

[3]Charles University, Faculty of Mathematics and Physics, 18000 Prague 8, Czech Republic

(Received 30 December 2016; revised 16 June 2017; accepted 19 June 2017)

The paper is devoted to the shapes of the solar wind ion flux fluctuation spectrum at the transition between the inertial and the kinetic range using *in situ* high-resolution measurements of the Russian mission Spektr-R. We analyse the variability of the transition region and select five typical types of spectral shapes: (i) spectra with two slopes and one break, (ii) spectra characterized by a nonlinear steepening in the kinetic range, (iii) spectra with flattening in the vicinity of the break, (iv) spectra with a bump in the vicinity of the break and (v) spectra without any steepening in the kinetic range. The most popular is the well-known type (i) observed in approximately half of the cases. The second most popular type of spectra is type (iii) occurring in approximately one third of the cases. The other three types are observed less often: type (ii) – in approximately 6 %; type (iv) in 3 % and type (v) in 6 % of cases. An analysis of typical plasma conditions for different types of spectra revealed that the last two type of spectra (iv) and (v) are generally observed in a very slow solar wind with a low proton density, (i) and (iii) are observed in the solar wind with rather typical conditions and (ii) is usually observed in high-speed streams. The effect of nonlinear steepening of the spectra in the kinetic range increases with the solar wind speed. We present also the analysis of statistical properties of the observed events and compare them with the predictions of several statistical turbulence models. We show that intermittency is always observed in the solar wind flow despite the presence of one or another shape of spectra. The log-Poisson model with a dominant contribution of filament-like structures shows the best parameterization of the experimentally observed scaling.

Key words: plasma properties, space plasma physics

1. Introduction

Investigations of the turbulent characteristics of the solar wind have acquired relevance during recent years. This interest is related to the problem of plasma heating owing to dissipation processes of turbulent fluctuations (see the review of

† Email address for correspondence: orearm@gmail.com

Matthaeus & Velli 2011). The energy is transferred between the range of the energy source and the dissipation range through a turbulent cascade (Goldstein, Roberts & Matthaeus 1995). The turbulent cascade can develop from the magnetohydrodynamic (MHD) regime (Biskamp 1994) down to the scales where kinetic effects should be considerable. Spectra of the interplanetary magnetic field in the so-called inertial range (MHD scale) typically tend to follow the power-law shape with a near-Kolmogorov slope $\sim -5/3$ (Bruno & Carbone 2013) as was predicted by Goldreich & Sridhar (1995). The spectra of plasma parameters often follow different laws. The bulk velocity spectra have a less steep slope $\sim -3/2$ (Grappin, Velli & Mangeney 1991; Podesta, Roberts & Goldstein 2006; Borovsky 2012; Šafránková *et al.* 2013*a*,*b*, 2016). The density spectra generally follow a power law with a slope similar to the slope of the magnetic field spectra (e.g. Neugebauer, Wu & Huba 1978; Marsch & Tu 1990) or steeper (down to -1.8 on average) slope than the magnetic field (Šafránková *et al.* 2013*b*, 2015). The slope of the spectra of the ion flux fluctuations (which is related to the density and the bulk velocity fluctuations) lies within a rather wide range, however, the mean slope is also near $\sim -5/3$ (Riazantseva *et al.* 2015). Spectra of turbulence observed in the solar wind become steeper at the kinetic scales (Alexandrova *et al.* 2013) and follow a power law with a slope of –(2.7–2.9) for the frequency spectra of the interplanetary magnetic field (e.g. Smith *et al.* 2006; Alexandrova *et al.* 2009), of the electron density (e.g. Chen *et al.* 2012), of the proton density (Šafránková *et al.* 2015), of the ion flux (Riazantseva *et al.* 2015) and also of the bulk velocity (Šafránková *et al.* 2016). Kinetic Alfvén or whistler turbulence is generally considered to be the reason of the spectrum steepening at high-frequency scales (Goldstein *et al.* 1995; Galtier 2006; Howes *et al.* 2008; Sahraoui *et al.* 2009; Schekochihin *et al.* 2009; Podesta 2013). The transition region is traditionally studied by introducing the frequency of the ion spectral break. Several studies try to find the relation of the break frequency of the magnetic field fluctuations to ion characteristic scales. Some of them argue that the break should be related to the ion cyclotron frequency f_c where the cyclotron damping of Alfvén waves starts (Goldstein *et al.* 1995; Leamon *et al.* 1998), other group suggests a relation to the ion Larmor radius ρ following from the kinetic Alfvén wave turbulence conception (Schekochihin *et al.* 2009; Boldyrev & Perez 2012). Others (e.g. Galtier 2006; Servidio *et al.* 2007) consider a relation with the ion inertial length λ ($\lambda = c/\omega_p$; c-the speed of light; ω_p-proton plasma frequency) because the dispersive Hall effect becomes important at shorter scales. However, the break frequency is not correlated with only one ion characteristic scale as has been supposed in numerous studies (Leamon *et al.* 1998; Smith *et al.* 2006; Markovskii, Vasquez & Smith 2008; Perri, Carbone & Veltri 2010; Bourouaine *et al.* 2012). Šafránková *et al.* (2015) proposed the concept of gyrostructure frequency ($f_\rho = V_p/2\pi\rho$; V_p – the solar wind bulk velocity, ρ – thermal gyroradius) which shows a rather good correlation with the break frequency for the spectra of the density fluctuations. Such a frequency would be observed if the structures of thermal gyroradius size move past the spacecraft in the solar wind. For the spectra of the bulk velocity fluctuations (Šafránková *et al.* 2016) the best correlation was shown for combination of the gyrostructure and the inertial length frequency ($f_\lambda = V_p/2\pi\lambda$).

Turbulence in the solar wind is in a non-equilibrium state and the mechanisms responsible for spectrum shaping are not yet completely clear (Howes *et al.* 2008). The spectrum is governed by complex processes of nonlinear interactions of waves leading to a development of kinetic plasma instabilities (e.g. Leamon *et al.* 1998; Gary 2015). The anisotropy observed in the solar wind is the main source of these instabilities (Gary 2015). Consequently, the specific plasma conditions in

https://doi.org/10.1017/S0022377817000502 Published online by Cambridge University Press

different solar wind types can lead to the formation of different spectra shapes (Bruno & Carbone 2013). For example, the 'bumps' near the spectral 'knee' can be due to Alfvén ion cyclotron waves (Alexandrova 2008), and the flattening in the high-frequency part of the spectra can be a result of whistler waves (Klein, Howes & Tenbarge 2014). Coherent structures and sharp discontinuities can also play an important role in the formation of the spectral shape (e.g. Lion, Alexandrova & Zaslavsky 2016). Such structures in the solar wind turbulence are a manifestation of spatial intermittency which is beyond the Kolmogorov phenomenology. The analysis of higher-order statistics always shows a high level of intermittency in the solar wind flow (Marsch & Tu 1997; Bruno & Carbone 2013). The fluctuations in the solar wind are distributed non-uniformly in space with scale-dependent non-Gaussian statistics. This can complicate the energy transfer across the scales of turbulence spectra. Coherent structures which concentrate the dissipation in their vicinity play a dominant role in the processes of plasma heating in current theoretical approaches (Matthaeus *et al.* 2015). The characteristics of the statistical properties of the turbulent flow can provide important information on turbulent energy dissipation processes and on the nature of turbulence. The spatial configuration of solar wind structures are at the base of the models predicting realistic shapes of spectra (Zelenyi & Milovanov 2004; Boldyrev & Perez 2012).

Experimental investigations of the spectrum in the dissipation range and in the transition region are still relevant. Recent investigations are based mainly on high-frequency measurements of the interplanetary magnetic field fluctuations (Alexandrova *et al.* 2013) because plasma measurements with a temporal resolution sufficient for an analysis around the ion scales are still rare. Several papers discussed particular spectra of the high-frequency electron density fluctuations (Celnikier *et al.* 1983; Kellogg & Horbury 2005; Chen *et al.* 2012) and the ion flux fluctuations (Unti, Neugebauer & Goldstein 1973). In this paper, we use systematic direct measurements of the ion flux fluctuations with high time resolution up to 30 ms provided by the Bright Monitor of the Solar Wind (BMSW) instrument on board of the Spektr-R spacecraft. This experiment (Šafránková *et al.* 2013*b*, 2015, 2016; Riazantseva *et al.* 2015, 2016; Rakhmanova, Riazantseva & Zastenker 2016; Rakhmanova *et al.* 2017) allows us to expand our knowledge on processes in the dissipation range and in the transition region. The relevance of this investigation is even increased by the fact that BMSW is a prototype of the Faraday cup (FAR) instrument which is proposed for high-resolution plasma measurements within the planed ESA THOR mission (Vaivads *et al.* 2016).

We present the statistics of observations of different features of the turbulence spectra in the transition region between MHD and kinetic scales. We define the most frequently observed shapes of spectra such as: (i) spectra with two clear slopes and one break, (ii) spectra with nonlinear steepening in the kinetic range without a clear break, (iii) spectra with a flattening in the vicinity of the break, (iv) spectra with a bump in the vicinity of the break, (v) spectra without noticeable steepening in the kinetic range. We analyse the proportion between different kinds of spectra shapes and identify specific conditions in the solar wind under which they are observed. Also, we discuss the universal statistical properties of turbulent fluctuations in the solar wind which do not depend on the spectral shape.

2. Measurements and methods

The BMSW instrument on board the high apogee Spektr-R spacecraft (astrophysical Russian mission) can provide measurements of the ion flux vector, proton density,

https://doi.org/10.1017/S0022377817000502 Published online by Cambridge University Press

bulk and thermal velocity in the solar wind and in the Earth's magnetosheath with time resolution up to 32 ms. The main axis of the instrument is oriented along the Sun–Earth line within the limits ±5–10°. The deviation angle of the device axis from the Sun–Earth line can be determined with a special solar sensor (DSS) with an accuracy of 1°. BMSW measurements are based on six Faraday cups. Three sensors are declined from the main axis of the instrument to determine the ion flux direction. Three other sensors are intended for measurements of the basic plasma moments under a Maxwellian approximation. The ion moments can be determined with time resolution ≈32 ms only part of the time (in adaptive mode) the rest of the time the integral energy distribution function and its moments are determined with a time resolution of ≈3 s (sweeping mode). However, the ion flux vector can be measured with the highest time resolution during the whole time of instrument operation. A more detailed description of the instrument principles can be found in Zastenker *et al.* (2013), Šafránková *et al.* (2013*a*). The time resolution of BMSW data is sufficient for the analysis of turbulent properties of the ion plasma fluctuations up to 16 Hz. We select several periods of the continuous ion flux measurements in the solar wind with duration longer than 3 h. We use also Wind data because magnetic field measurements are missed on Spektr-R. We try to select intervals as long as possible, but we are limited by the Spektr-R telemetry because only 10 % of full time resolution measurements are transmitted to the Earth.

The selected periods are divided into ≈17 min subintervals (note that a number of data points expressed by a degree of two is favourable for a Fourier analysis and we use $2^{15} = 32\,768$ points in each interval). The requirement of stationarity limits the usage of longer intervals. The length of the intervals is enough to analyse the spectra in the frequency range of 0.01–16 Hz but we use the frequency range only up to 10 Hz because results of the in-flight calibration and laboratory tests show that the noise level can be significant for frequencies higher than 8–10 Hz (Šafránková *et al.* 2013*b*; Chen *et al.* 2014*a*). Nevertheless, longer intervals can be used to clarify the shape of the spectrum. Intervals are overlapped by half of the interval length and we analyse approximately 700 of such intervals. Frequency spectra are calculated for each interval by the fast Fourier transform (FFT) method smoothed in the frequency domain (with the use of a Hamming window) and sorted by shape using an automated routine based on spectral slopes. The selection is checked manually.

Our selection is not limited to the pristine solar wind. We further sort our intervals in accordance with the catalogue of Yermolaev ftp://ftp.iki.rssi.ru/pub/omni/catalog/ (Yermolaev *et al.* 2009) and we note that our set consists of nearly equal proportions of three types of solar wind: (i) slow solar wind regions (∼40 % of the time); (ii) regions of interplanetary coronal mass ejections ('EJECTA') (or complex phenomena such as compressed regions inside EJECTA-like events) (∼30 % of the time); and (iii) compression regions before high-speed streams, so-called corotating interaction regions (CIR), and before EJECTA or magnetic clouds (MC), so-called SHEATH regions (CIR and SHEATH regions are observed ∼30 % of the time). MCs are not included in our statistics because they are less common (Yermolaev *et al.* 2009). The instrument limitation of the velocity measurements of up to ∼600–700 km s^{-1} do not allow us to observe the high-speed streams.

The averaged values of plasma parameters are calculated for each interval of the BMSW measurements (the proton density N_p, the bulk velocity V_p, the proton temperature T_p, the alpha density N_α and the relative abundance of helium N_α/N_p with 3 s time resolution). As it was noted above, data from a magnetometer are not available on board Spektr-R. However, the magnetic field magnitude B is determined

https://doi.org/10.1017/S0022377817000502 Published online by Cambridge University Press

for each interval from Wind measurements shifted to the position of Spektr-R (Wind data are downloadable from the CDAWeb data base). This allows us to determine also other parameters which are often considered as affecting the properties of turbulence: the Alfvén velocity V_A, the proton plasma beta β_p, the cyclotron frequency f_c, the proton gyroradius ρ, the inertial length λ, the inertial length frequency f_λ and the gyrostructure frequency f_ρ (see § 1).

According to the Taylor hypothesis, the observed ion flux variations in the solar wind can be considered as the spatial variations passing by the spacecraft with the bulk velocity. To confirm the possibility of application of the Taylor hypothesis we always test the ratio of V_p/V_A. The mean value of this ratio is ∼10 for our statistics. We rejected the cases with $V_p/V_A < 3$. It is known that the Taylor hypothesis can be violated in the case of quasi-parallel propagating whistler waves (e.g. Klein *et al.* 2014). We exclude the intervals suspected as foreshocks, where whistler waves are mainly observed. We assume that the possible influence of whistler waves on the solar wind turbulence is rather weak (Alexandrova *et al.* 2008).

The statistical properties of the ion flux fluctuations (such as probability distribution functions, their high-order structure functions, moments and scaling) are also analysed for the same time intervals (details will be explained in § 5).

3. Variability of the shapes of the ion flux fluctuation spectra at the ion scales

Spectra of the plasma fluctuations in the kinetic range can always differ strongly from the spectra at the MHD scale (see § 1). The character of these distinctions can vary for different observation intervals at different plasma conditions (Bruno & Carbone 2013). In this section, we present several examples of different shapes of spectra and in the next section we compare statistically the plasma parameters typical for different types of spectra.

Usually a significant number of fluctuation spectra in the solar wind can be well fitted by power laws with different slopes in the MHD and in the kinetic ranges (Smith *et al.* 2006; Alexandrova *et al.* 2009; Perri *et al.* 2010; Bourouaine *et al.* 2012; Šafránková *et al.* 2013*a*,*b*; Riazantseva *et al.* 2015). In this case, the power-law ranges are divided by a clear break point. This type of spectrum is observed in ∼50 % of the solar wind intervals analysed in our statistics. Below we will call them spectra with two slopes and one break.

Figure 1(*a*) presents an example spectrum of the solar wind ion flux fluctuations observed on 2nd August 2012 12:44-13:01 UT that exhibits two slopes and one break. The mean values of plasma parameters during this period are: the ion density $N_p = 12$ cm^{-3}, the plasma bulk velocity $V_p = 406$ km s^{-1}, the proton temperature $T_p = 13$ eV, the interplanetary magnetic field magnitude $B = 10$ nT, the Alfvén velocity $V_A = 66$ km s^{-1}, the proton plasma beta $\beta_p = 0.6$, the cyclotron frequency $f_c = 0.15$ Hz, the proton gyroradius $\rho = 51$ km, the proton inertial length $\lambda = 68$ km, the inertial length frequency, $f_\lambda = 0.95$ Hz, the gyrostructure frequency $f_\rho = 1.3$ Hz. Two clear power-law parts of the spectrum with slopes $P_1 = -1.62$ at the MHD frequency scales, and $P_2 = -2.67$ at higher frequencies, are observed. In Riazantseva *et al.* (2015), we have analysed spectra with two slopes and one break separately and have shown that the average slope in the kinetic range is equal to $\sim\langle P_2\rangle = -2.9$, which is rather typical for the fluctuations of other plasma parameters such as density and bulk velocity observed on board Spektr-R (Šafránková *et al.* 2013*a*,*b*, 2016) as well as for the plasma and the magnetic field fluctuations observed in numerous other experiments (see the review of Alexandrova *et al.* (2013)). Less steep slopes can be observed if

https://doi.org/10.1017/S0022377817000502 Published online by Cambridge University Press

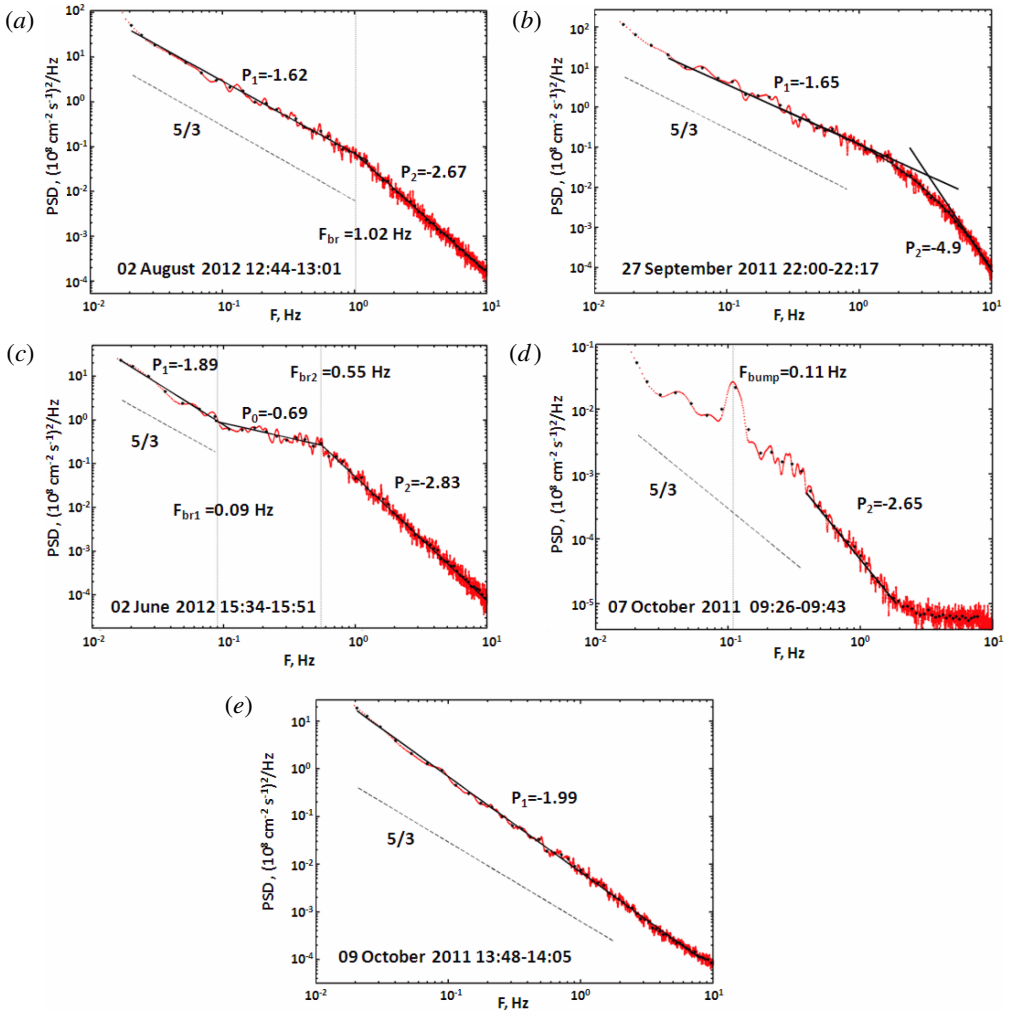

FIGURE 1. Examples of different spectral shapes of the ion flux fluctuations in the solar wind: spectra with two slopes and one break (*a*), spectra with nonlinear steepening in the kinetic range (*b*), spectra with flattening in the vicinity of the break (*c*), spectra with bump in the vicinity of the break (*d*), spectra without steepening in the kinetic range (*e*). Black lines show the linear approximation of different areas of spectra. A power law with slope $-5/3$ (Kolmogorov slope) is shown in all graphs by an oblique dotted line. Vertical dotted lines correspond to the frequencies of breaks or peaks.

the dissipation is weakened (e.g. Smith *et al.* 2006). The break in figure 1(*a*) is determined as the intersection of the slopes obtained by independent linear fits of the lower (MHD) and upper the (kinetic) frequency range (e.g. Bourouaine *et al.* 2012). The frequency of the break is equal to $F_b = 1.02$ Hz which is ~ 7 times greater than the cyclotron frequency f_c, and is approximately equal to the inertial length frequency f_λ. It seems reasonable and in accordance with the relationship of the break frequency in the spectra of the magnetic fluctuations with the inertial length for low plasma β_p (Chen *et al.* 2014*b*). In Riazantseva *et al.* (2015), we have shown that the break frequency for the ion flux fluctuation spectra varies in a wide range and equals on

https://doi.org/10.1017/S0022377817000502 Published online by Cambridge University Press

average to $\langle F_b \rangle = 1.9 \pm 0.8$ Hz. Taking into account the dispersion, this value agrees well with the break frequency for the ion density fluctuations ~1.6 Hz (Šafránková *et al.* 2013*b*) and the electron density fluctuations (~1 Hz, Chen *et al.* (2012)). The break frequency of the spectrum of the velocity fluctuations (Šafránková *et al.* 2016) is smaller (~0.4 Hz) in comparison with the break of the density spectra and this difference tends to decrease with β. The experimental observations of the magnetic field fluctuations also show a large dispersion of the break frequency ~0.1–0.7 Hz (see review of Alexandrova *et al.* (2013)). The experimentally observed spectra of the fluctuations of the plasma or the magnetic field do not allow us to establish an unambiguous correlation of the break frequency of one of the plasma characteristic scales (see discussion in § 1). The selection of the main physical processes controlling the break is a complex problem which also has to take into account the different contributions of coherent structures, waves and non-coherent fluctuations which can influence the spectrum formation for different plasma parameters (Lion *et al.* 2016). These factors can probably explain the formation of spectra shapes differing from those discussed above.

The steepening of the spectrum in the kinetic range does not always follow a power law. The second type of spectrum under consideration is a spectrum with nonlinear steepening in the kinetic range. Figure 1(*b*) is a typical example of a spectrum of this type that was observed on 27 September 2011 22:00-22:17 UT. The mean plasma parameters during this period were: $N_p = 18$ cm^{-3}, $V_p = 553$ km s^{-1}, $T_p = 5$ eV, $B = 7$ nT, $V_A = 34$ km s^{-1}, $\beta_p = 0.9$, $f_c = 0.1$ Hz, $\rho = 52$ km, $\lambda = 54$ km, $f_\lambda = 1.6$ Hz, $f_\rho = 1.7$ Hz. So the discussed event is observed in a rather fast and dense solar wind. The traditional linear fit shows that a clear break point is not observed. The spectrum is smoothly descending while the slope of the spectrum is growing toward higher frequencies and reaching a very high value of $P_2 = -4.9$, whereas the power-law slope at the MHD scale is equal to the typical value $P_1 = -1.65$. The spectrum begins to steepen at 1–2 Hz which is close to both the inertial length and the gyrostructure frequencies (they are approximately equal to each other because of $\beta_p \sim 1$). It is necessary to stress that the mean velocity during this period is rather high and we can say that this type of spectrum is typically observed in the fast solar wind. This corresponds well to Pitňa *et al.* (2016) who showed that the ion density spectra fall faster downstream of interplanetary shocks, where the value of the velocity is always large. We also see the nonlinear rapid steepening of the spectrum in high-velocity streams not associated with shocks. At the same time, Bruno, Trenchi & Telloni (2014*a*) have shown non-power-law smooth transition for the spectrum of the interplanetary magnetic field fluctuations, and also the faster fall of the spectrum slope with growing solar wind velocity. We observe this type of spectrum only for 6 % of the intervals. A small number of the observed spectra are probably connected to the small number of intervals with a high value of the velocity in our statistics. The exponential fall was predicted in the dissipation range for ordinary fluid flows (Frisch 1995) and also for the solar wind plasma (Howes *et al.* 2008). The exponential descent of the spectrum of the interplanetary magnetic field fluctuations is observed often in a transition from ion to electron scales and can usually be associated with acceleration of the dissipation processes (Alexandrova *et al.* 2009).

Sometimes the transition region can be characterized by a more complex spectrum with a plateau between the MHD and the kinetic ranges instead of clear break. Below we call them spectra with a flattening in the vicinity of the break. Figure 1(*c*) represents an example of this spectrum observed on 2 June 2012 15:34–15:51 UT.

https://doi.org/10.1017/S0022377817000502 Published online by Cambridge University Press

The mean plasma parameters during this period are: $N_p = 22$ cm^{-3}, $V_p = 354$ km s^{-1}, $T_p = 3$ eV, $B = 4$ nT, $V_A = 20$ km s^{-1}, $\beta_p = 1.6$, $f_c = 0.06$ Hz, $\rho = 62$ km, $\lambda = 50$ km, $f_\lambda = 1.1$ Hz, $f_\rho = 0.9$ Hz. The spectrum in the figure is fitted by three power laws, the intersection of them gives two break points. The spectrum flattens at the scale ~0.1–0.6 Hz, and can be approximated by a power law $P_1 = -1.89$ before the flattening (at the end of the MHD scale) and by a power law $\langle P_2 \rangle = -2.83$ after the flattening. The slope of the flatter part is equal to $\langle P_0 \rangle = -0.69$. The first break point separates the MHD scale from the transition scale with the flattening. It is equal to $F_{br1} = 0.09$ Hz which is of the same order as the cyclotron frequency f_c. The second break is equal to $F_{br2} = 0.55$ Hz, which is close to the gyrostructure frequency. We need to take into account that the gyrostructure frequency is slightly lower than the inertial length frequency because β_p is only slightly greater than unity. As it was shown in Šafránková *et al.* (2015) that the gyrostructure frequency is the best scaling parameter for the location of the second break point of a similar density fluctuation spectra. It reflects the strong changes of character of the turbulence at scales comparable to the proton gyroradius. Chen *et al.* (2014*b*) have shown that the break in the magnetic field fluctuation spectrum can be associated with the gyrostructure frequency only for high β_p (as for the spectrum in figure 1*c*), whereas low β_p determines the relationship to the inertial length (as for the spectrum presented above in figure 1*a*). The plasma β_p parameter also influences the width of the flatter region, which tends to decrease with increasing β_p (Šafránková *et al.* 2016). The significant interrelation of the characteristics of spectra and plasma β is connected with the effect of β on the compressibility of the system (Servidio *et al.* 2015). The spectra with the flattening are observed often for the ion density fluctuations (Šafránková *et al.* 2013*a*,*b*, 2015; Chen *et al.* 2014*a*). The ion flux fluctuations considered in the current paper are mainly density fluctuations and exhibit a similar spectrum (Pitňa *et al.* 2016). The spectra with flattening are observed rather often but not always, in 32 % of intervals in the solar wind. Similar flattening around ion scales of the spectrum was first observed by Unti *et al.* (1973) for the ion flux fluctuations and by Celnikier *et al.* (1983), Kellogg & Horbury (2005) and Chen *et al.* (2012) for the electron density fluctuations. Several authors attributed the flattening to the temperature anisotropy instabilities (Neugebauer *et al.* 1978) or to the dominance of kinetic Alfvén waves (e.g. Chandran *et al.* 2009).

Sometimes the spectra of the ion flux fluctuations (of all above types) can be further distorted by a distinct peak with maximum in the transition region between the MHD and the kinetic ranges. Hereafter we call them spectra with a bump in the vicinity of the break. Figure 1(*d*) demonstrates the spectra of the ion flux fluctuations for the interval 7 October 2011 09:26–09:43 UT. The mean plasma parameters during this period are: $N_p = 5$ cm^{-3}, $V_p = 393$ km s^{-1}, $T_p = 1$ eV, $B = 3$ nT, $V_A = 27$ km s^{-1}, $\beta_p = 0.4$, $f_c = 0.04$ Hz, $\rho = 65$ km, $\lambda = 107$ km, $f_\lambda = 0.6$ Hz, $f_\rho = 1$ Hz. So this event presents the lowest plasma parameters in comparison with other examples discussed in the paper. The peak is visible at a frequency of $F_{bump} = 0.11$ Hz between the cyclotron frequency f_c and the inertial length frequency f_λ. It seems that the bump is located in the background of a spectrum of the third type (spectrum with flattening in the vicinity of the break). It is difficult to determine break(s) in this case but the second break F_{br2} seems to be equal to ~0.4 Hz (see figure 1*d*). The break is again near the inertial length frequency as was shown by Chen *et al.* (2014*b*) for low β_p. The slope of the spectra at frequencies higher than F_{br2} is equal to $P_2 = -2.65$ that is typical for the kinetic range. The flattening at frequencies exceeding 2 Hz can be explained by a low level of density fluctuations (10 times lower than that in the previous figures)

https://doi.org/10.1017/S0022377817000502 Published online by Cambridge University Press

that does not exceed the noise level. The spectra with a bump can be observed only in 3 % of cases in the solar wind (only ∼20 of the spectra in our statistics), they can be observed more frequently in the magnetosheath (see the paper of Rakhmanova *et al.* (2017) in the current issue). The similar bumps observed in the area of the spectral break are typical for the magnetic field fluctuations in the magnetosheath and they can be associated with Alfvén vortices (Alexandrova 2008). Roberts *et al.* (2016) proved the possibility of the existence a quasi-monopolar Alfvén vortex in the solar wind but the low value of Alfvén velocity in our example and the absence of magnetic field data make it difficult to use the same approach in our investigation.

The last type of spectra is the spectrum without steepening in the kinetic range. Figure 1(*e*) demonstrates an example of such a spectrum observed on 9 October 2011, 13:48-14:05 UT with one slope and without a visible break in the frequency spectrum. The mean plasma parameters during this period are: $N_p = 10$ cm^{-3}, $V_p = 321$ km s^{-1}, $T_p = 3$ eV, $B = 6$ nT, $V_A = 39$ km s^{-1}, $\beta_p = 0.3$, $f_c = 0.09$ Hz, $\rho = 42$ km, $\lambda = 73$ km, $f_\lambda = 0.7$ Hz, $f_\rho = 1.2$ Hz. We can identify only one slope that is rather steep ($P = -1.99$) in the inertial range but is too gradual in the kinetic range. It should be taken into account that we can see here only the high-frequency end of the inertial range which is not necessarily enough for the slope determination. The spectral slope at the MHD scale can be as high as -2 when, for example, the local magnetic field direction is parallel to the flow (Horbury, Forman & Oughton 2008). However, the spectrum should steepen in the kinetic range even in these cases. As was shown (Riazantseva *et al.* 2015; Šafránková *et al.* 2015), the slope of the kinetic part of the spectrum can vary over a wide range. The low slopes can be a sign of reduced dissipation (Smith *et al.* 2006). In Klein *et al.* (2014) whistler waves are considered as the possible reason of the spectral flattening in the high-frequency range. In that case, we cannot see the difference between the MHD and the kinetic ranges and identify the location of the break point. The latest type of spectrum is observed in only ∼6 % cases but this number cannot be ignored.

4. Statistical distribution of plasma parameters associated with different types of spectra

The proportions between different shapes of spectra and the mean plasma parameters for each of them are summarized in table 1. Each row of the table corresponds to one of the types discussed above. The remaining ∼2.6 % of spectra with a more complicated shape were not included into the table. Distributions of plasma parameters shown in figure 2 for all types of spectra correspond to the typical values encountered in the solar wind but several interesting features can be pointed out for certain types of spectra. The distribution of the proton density does not show any significant difference for the different types of spectra. The mean value of the proton density is a bit higher for spectra of type 1 and type 2, $\langle N_p \rangle \approx 14$–$15$ cm^{-3}, whereas the three other types were found to be at densities of $\langle N_p \rangle \approx 10$–$12$ cm^{-3}. This difference is caused by a number of the spectra corresponding to a rather high value of proton density $N_p > 30$ cm^{-3} in the first two groups. A similar situation is observed also for helium density N_α: largest mean values of helium density for type 2 spectra $\langle N_\alpha \rangle = 0.8$ cm^{-3} are associated with a distribution tail with high values of $N_\alpha > 0.6$ cm^{-3}. This is clearly seen for the distribution of relative helium abundance N_α/N_p (figure 2*d*): a significant number of intervals with a high value of $N_\alpha/N_p \sim 7$–10 % characterize type 2 spectra. The mean value of relative helium abundance for the second group of spectra is equal to $\langle N_\alpha/N_p \rangle \approx 6$ %, but the

https://doi.org/10.1017/S0022377817000502 Published online by Cambridge University Press

Number of type	Type of spectrum shape	Relative amount (%)	N_p (cm^{-3})	N_α (cm^{-3})	N_α/N_p (%)	T_p (eV)	V_p (km s^{-1})	V_A (km s^{-1})	B (nT)	β_p
1.	Spectra with two slopes and one break	49.6	14.3	0.48	3.6	4.5	446.7	49.0	7.8	0.95
2.	Spectra with non-linear steepening in the kinetic range	6.3	15.6	0.78	5.8	6.5	528.1	61.4	10.1	0.89
3.	Spectra with flattening in the vicinity of the break	32.3	12.0	0.33	3.1	4.6	433.7	61.7	8.5	0.65
4.	Spectra with a bump in the vicinity of the break	3.1	11.4	0.25	2.3	3.5	372.0	38.0	5.3	0.60
5.	Spectra without steepening in the kinetic range	6.1	10.6	0.38	3.1	3.0	373.0	43.6	5.7	0.86

TABLE 1. The mean values of plasma parameters for different shapes of spectra.

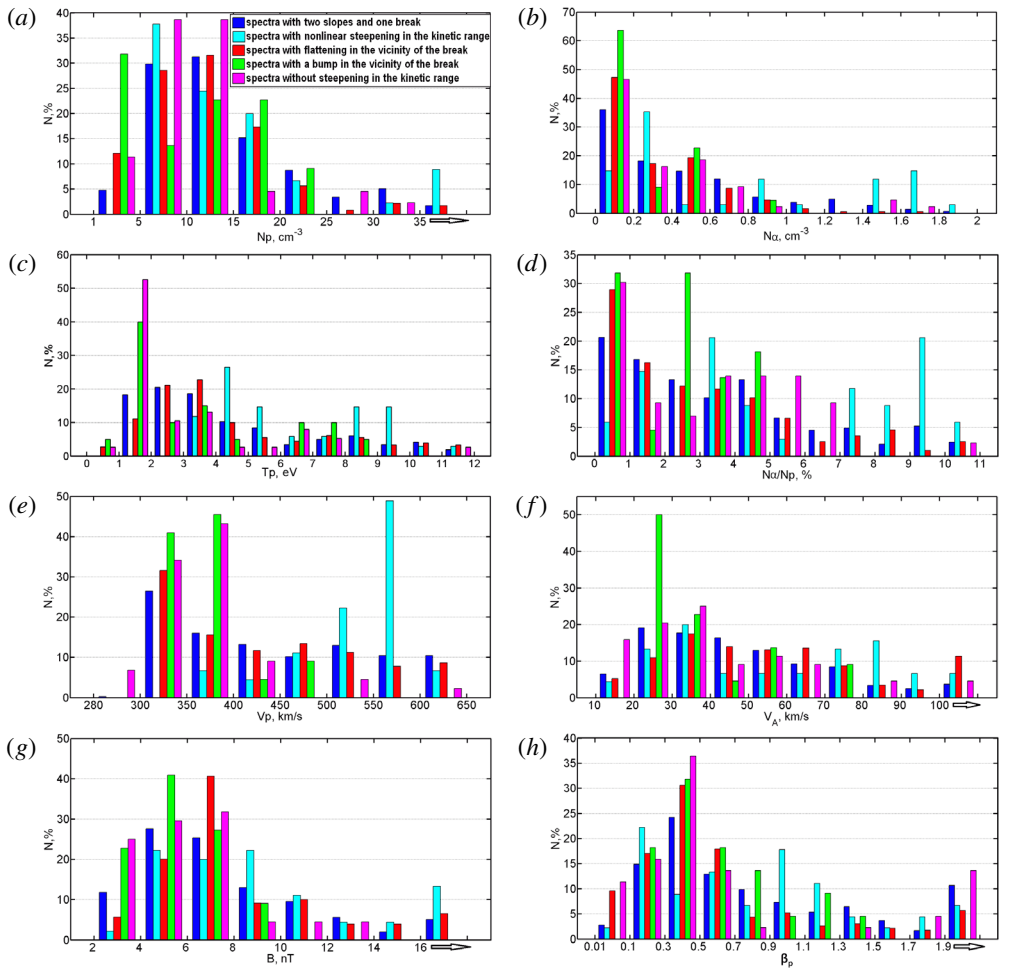

FIGURE 2. Distributions of solar wind parameters: the proton density N_p (*a*), the helium (α particle) density N_α (*b*), the proton temperature T_p (*c*), the helium abundance N_α/N_p (*d*), the bulk velocity V_p (*e*), the Alfvén velocity V_A (*f*), the magnetic field magnitude B (*g*) and the proton plasma parameter β_p (*h*) for different types of spectra. The arrows on panels (*a,f,g* and *h*) show that the last bins combine all values of the largest amplitude of the current parameter (greater than the left border of the bin).

distribution contains two clear separated parts: approximately half of the spectra are characterized by high helium abundance $N_\alpha/N_p > 7\,\%$, the other half lie in the limits $\sim$1–5 %. The temperature distribution shows a large dispersion (figure 2*c*).

The majority of intervals shows T_p within in the limits $\sim$1–4 eV, but the mean value is greater as a result of the contribution of intervals with hotter plasma. The distribution for type 4 and type 5 spectra shows the maximum at a rather low temperature ($T_p \sim$ 1–2 eV) with the shifted mean value $\langle T_p \rangle \approx$ 3–3.5 eV.

The distribution for type 1 and type 3 spectra exhibits a maximum at temperature $T_p \sim$ 1–4 eV with shifted mean value $\langle T_p \rangle \approx 4.5$ eV. The distribution for type 2 spectra is shifted to higher temperatures, its mean value $\langle T_p \rangle \approx 6.5$ eV. In view of wide variations of the temperature distribution, the difference between groups cannot be

https://doi.org/10.1017/S0022377817000502 Published online by Cambridge University Press

considered sufficiently reliable. The clearest result is seen for the distribution of the bulk velocity (figure 2*e*). The distribution for type 2 spectra shows the significantly higher values of bulk velocity $V_p \sim 500$–600 km s^{-1} than the distribution for the other types of spectra ($V_p \sim 300$–400 km s^{-1}). The mean values of $\langle V_p \rangle$ are equal to $\langle V_p \rangle \approx 530$ km s^{-1} for type 2 spectra, $\langle V_p \rangle \approx 430$–$450$ km s^{-1} for type 1 and type 3 spectra, $\langle V_p \rangle \approx 370$ km s^{-1} for type 4 and type 5 spectra. The mean value of the bulk velocity V_p for type 1 and type 3 spectra is caused by the elongated tail of the distribution. The distribution of Alfvén velocity varies in a wide range for all types of spectra (figure 2*f*). Only type 4 spectra have a clearly distinguished peak at a low value of Alfvén velocity, $V_A \sim 20$–30 km s^{-1} (the mean value of the distribution is $\langle V_A \rangle = 38$ km s^{-1}).

The other types of spectra have a maximum of the distribution in the broader limits $V_A \sim 20$–50 km s^{-1}. The mean value of the Alfvén velocity for type 1 and type 5 spectra is equal to $\langle V_A \rangle \approx 40$–$50$ km s^{-1}, whereas it's mean value for type 2 and type 3 spectra is $\langle V_A \rangle \approx 60$ km s^{-1} because of the presence of a rather large amount of spectra with a comparatively large value of V_A(>50 km s^{-1}). The magnetic field distribution (see figure 2*g*) for all types of spectra except type 2 has a maximum at $B \sim 2$–6 nT with mean values $\langle B \rangle \approx 8$ nT for type 1 and type 3 spectra and $\langle B \rangle \approx 5$ nT for type 4 and type 5 spectra. The distribution for type 2 spectra seems to be wider with a mean value of $\langle B \rangle \approx 10$ nT due to a number of spectra with large B (>16 nT). The distribution of plasma β_p does not show any significant difference among the groups of spectra (figure 2*h*). The majority of the spectra have $\beta_p < 0.9$ with a maximum at $\beta_p \sim 0.3$–0.5, except the intervals of type 2 that have two peaks: one at a lower value $\beta_p \sim 0.1$–0.3 and the second at $\beta_p \sim 0.9$–1.1. Meanwhile, a significant number of spectra with a high value of $\beta_p > 1.9$ is observed for type 1, type 2 and type 5 spectra, which leads to mean values $\langle \beta_p \rangle \approx 1$. On the other hand, the mean value of β_p for type 3 and type 4 spectra is equal to $\langle \beta_p \rangle \approx 0.6$.

The differences of the solar wind parameters for the various types of spectral shapes bring us to believe that these or other spectral shapes are connected with the individual type of solar wind. Table 2 presents the proportions of spectral shapes referring to the several types of the solar wind observed in the paper (see § 2).

The most numerous types of spectral shapes (type 1 and type 3) are observed in all types of the solar wind in approximately equal proportions. We can only note that in the pristine slow solar wind, the relative number of spectra type 3 is larger and approaches the relative number of spectra type 1. Also we can note that the spectra of type 2 and type 4 are often observed during 'EJECTA' or complex phenomena such as compressed regions inside EJECTA-like events, but the statistics for such subclassification is rather poor. More accurate analysis will be carried out in our subsequent works on more extensive statistical material.

5. Statistical properties of turbulence for different shapes of the ion flux fluctuation spectra in the solar wind

The traditional approach describes the behaviour of the fully developed isotropic turbulence (Kolmogorov 1941) and does not take into account a local breaking of turbulence homogeneity (so-called intermittency) considered first by Novikov & Stewart (1964). The statistical properties of intermittent flow strongly deviate from the statistics of the Kolmogorov model (K41). The statistical methods taking into account the probability distribution function (PDF) and its moments can better describe the properties of a turbulent medium. Intermittency is typically observed in space

https://doi.org/10.1017/S0022377817000502 Published online by Cambridge University Press

Spectral type	Type of spectrum shape	The pristine slow solar wind	Interplanetary coronal mass ejections ('EJECTA') (or complex phenomena such as compressed regions inside EJECTA-like events)	Compression regions before high-speed streams so-called CIR and before EJECTA or MC so-called SHEATH
1.	Spectra with two slopes and one break	43.5 %	51 %	56.2 %
2.	Spectra with nonlinear steepening in the kinetic range	4.2 %	9 %	6.4 %
3.	Spectra with flattening in the vicinity of the break	37.9 %	27.8 %	29.2 %
4.	Spectra with a bump in the vicinity of the break	2.8 %	4.7 %	1.8 %
5.	Spectra without steepening in the kinetic range	7 %	6.6 %	4.6 %

TABLE 2. The proportions of spectral shapes referring to different types of the solar wind.

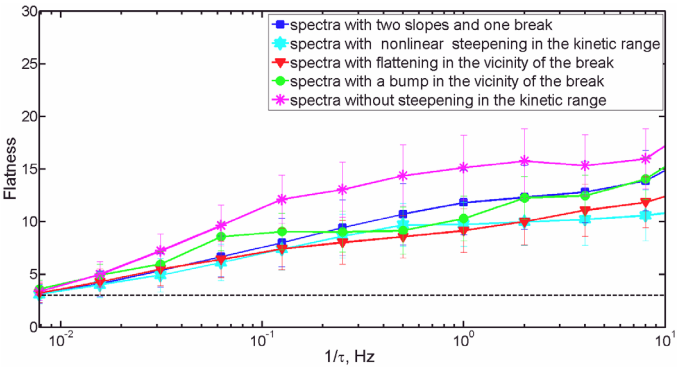

FIGURE 3. An average value of the fourth-order moment (flatness) for the PDF of the ion flux fluctuations versus scale parameter $1/\tau$ for different types of spectra.

experiments as non-Gaussian, scale-dependent statistics of parameters which lead to the breaking of trivial self-similarity (Marsch & Tu 1997; Bruno & Carbone 2013 and references therein). Fluctuations of parameters in the space plasma correspond usually to the presence of multifractality and self-similarity at all scales (Zelenyi & Milovanov 2004). Long-range correlations and memory effects observed in the cosmic plasma are the result of self-similarity and intermittency (Budaev, Savin & Zelenyi 2011). Statistical properties of turbulence follow the universal laws despite the various conditions in the plasma in different areas of the near-Earth space and also in laboratory plasma (Budaev *et al.* 2011; Budaev, Zelenyi & Savin 2015). We will show below that the solar wind ion flux fluctuations for different shapes of spectra have similar statistical properties. For each analysed interval, we calculate the PDF, high-order moments of the PDF and analyse their scaling. Then we compare the average statistical properties for each type of spectra defined in §§ 3 and 4.

Intermittency can be quantified by a growing of flatness (the fourth-order moment of the PDF which reflects the deviation from Gaussianity) toward smaller spatial scales (or high-frequency scales in the sense of frequency of variations) (Frisch 1995). Figure 3 presents the dependence of the flatness F of the ion flux fluctuations versus the time scale parameter $1/\tau$ for the groups of different shapes of spectra (where $F(\tau) = \langle(\mathrm{Flux}_i(t+\tau) - \mathrm{Flux}_i(t))^4\rangle / (\langle(\mathrm{Flux}_i(t+\tau) - \mathrm{Flux}_i(t))^2\rangle)^2$, τ ranges from 0.1 to 256 s). The dashed line corresponds to $F = 3$ for a Gaussian PDF. One can see a significant growing of flatness toward the kinetic scales that continues in the kinetic range with a smaller slope. The increase of non-Gaussianity toward the kinetic range was earlier observed for the magnetic field and bulk velocity fluctuations (Marsch & Tu 1997; Sorriso-Valvo *et al.* 1999; Bruno *et al.* 2003; Salem *et al.* 2009) and separately for the fluctuations of plasma parameters (Hnat, Chapman & Rowlands 2003; Riazantseva & Zastenker 2008; Riazantseva, Zastenker & Karavaev 2010; Bruno *et al.* 2014*b*). The statistical properties presented in these papers show a similar behaviour for the magnetic field and plasma fluctuations. The flatness continues to grow (Alexandrova *et al.* 2008; Kiyani *et al.* 2009; Yordanova *et al.* 2009; Riazantseva *et al.* 2015) or remains almost constant (Chen *et al.* 2014*a*) at kinetic scales. Riazantseva *et al.* (2016) have shown that flatness can vary in a broad range for different time intervals but, on average, it tends to grow up to a scale of ∼0.1 s for the ion flux fluctuations. The authors also show the presence of intermittency in the whole range of discussed scales. The behaviour of the flatness

https://doi.org/10.1017/S0022377817000502 Published online by Cambridge University Press

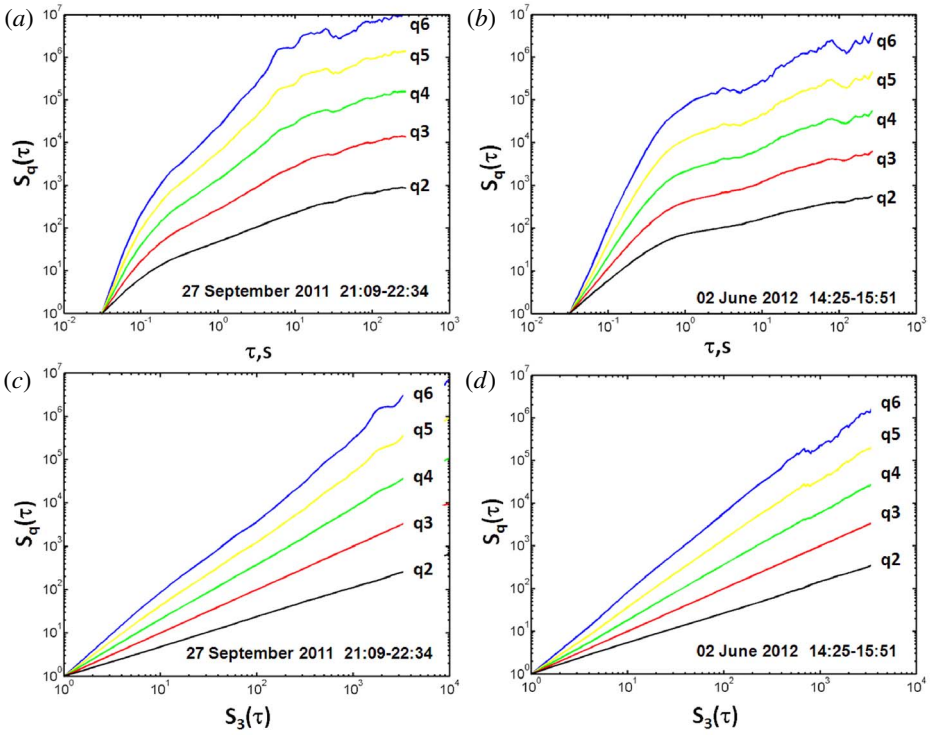

FIGURE 4. High-order structure function versus time scale τ (*a,b*) and versus the third-order structure function (*c,d*) for different types of spectra: spectra with nonlinear steepening in the kinetic range, 27 September 2011 21:09–22:34 UT (*a,c*); spectra with flattening in the vicinity of the break, 2 June 2012 14:25–15:51 UT (*b,d*).

for different types of spectra (shown by different colours and markers in figure 3) is similar but the fastest growing of $F(1/\tau)$ is observed for the group of spectra without steepening in the kinetic range. In general, the differences among the flatness profiles for different types of spectra are comparable with the statistical errors. It is necessary to take into account the qualitative character of the flatness dependence. It indicates the presence of intermittency but does not allow us to establish the precise quantitative difference of the intermittency level between different spectral types. Nevertheless, we can say that the intermittent flow is observed for all types of spectra, which is typical for a multifractal signal (Bruno & Carbone 2013). The scale invariance of the intermittent ion flux in the solar wind can be confirmed by analysis of the dependence of the high-order structure functions on the time scale parameter $\tau : S_q(\tau) = \langle|\mathrm{Flux}_i(t+\tau) - \mathrm{Flux}_i(t)|^q\rangle$. The nonlinear dependence $S_q(\tau)$ was shown by Riazantseva *et al.* (2015) for type 1 spectra (spectra with two slopes and one break). We present the nonlinear dependence of $S_q(\tau)$ for a wide range of scales for type 2 spectrum (spectra with nonlinear steepening in the kinetic range) in figure 4(*a*) and for the type 3 spectrum (spectra with flattening in the vicinity of the break) in figure 4(*b*). These figures present the structure functions up to order 6 (the analysis of higher orders is not statistically significant, Dudok de Wit *et al.* 2013). For analysis of the higher orders of the structure functions, we atempt to use longer intervals than we have used for the analysis of the spectra. For calculation

https://doi.org/10.1017/S0022377817000502 Published online by Cambridge University Press

of the structure functions in figure 4 we select periods during which when the same type of spectrum is observed over a rather long period of time (∼1.5 h). The selected intervals include the intervals presented in figure 1.

The observed dependences demonstrate strong deviation from a linear scaling $\zeta(q) = q/3$ typical for Kolmogorov turbulence (Kolmogorov 1941). The measured structure function power law $S_q(\tau) \sim \tau^{\zeta(q)}$ shows the nonlinear scaling $\zeta(q)$ and excludes a trivial self-similarity and scale invariance for the corresponding scales. It is a rather typical situation for the solar wind turbulent flow (Burlaga 1991; Hnat, Chapman & Rowlands 2005; Budaev *et al.* 2015). Herewith the extended self-similarity (ESS) can be shown by linear dependence of $\log(S_q(\tau))$ from $\log(S_3(\tau))$ (Benzi *et al.* 1993). The ESS is a universal property of statistical symmetry in the system of plasma turbulence in space, laboratory and even neutral fluids (Budaev *et al.* 2011) that leads to hidden statistical symmetries of the motion equations and multifractality. It provides the scale invariance of the process over a wide range of scales. This is clearly shown for almost two to three orders of magnitude $S_q(l)$ for spectra with a nonlinear descent in the kinetic range and spectra with a flattening in the vicinity of the break (see figure 4*c*,*d*). We do not show here the ESS plots for other types of spectra but they are always similar. In the solar wind plasma the ESS is observed predominately for the plasma fluctuations at inertial scales (Carbone, Veltri & Bruno 1995; Hnat *et al.* 2005). Recently, it was also shown to be the case for the ion flux fluctuations, including the kinetic range (Budaev *et al.* 2015; Riazantseva *et al.* 2015), but only for spectra with two slopes and one break.

The analysis of the experimental scaling $\zeta(q)$ can help to validate a preferred model of the intermittent turbulence (Budaev *et al.* 2011, 2015). The description of the observations of intermittent turbulence with the ESS can be implemented to the log-Poisson turbulence models. These models are a generalization of fractal models of turbulence with intermittency (Dubrulle 1994; She & Leveque 1994).

Figure 5 demonstrates typical examples of comparison of normalized experimental scaling $S_3(l)^{\zeta(q)/\zeta(3)}$ of the PDF in the solar wind flow with a linear scaling $q/3$ for the K41 (Kolmogorov) model (dashed blue line) and with the predictions of the models of turbulence with intermittency: She–Leveque model (solid line) and Biskamp–Mueller model (dotted line). Different colours and marks show different subintervals with several types of spectra. The intervals correspond to the following types of spectra: spectra with two slopes and one break correspond to intervals 1.1, 1.2, 1.3 in figure 5(*a*) and intervals 2.1, 2.2 in figure 5(*b*); spectra with nonlinear steepening in the kinetic range correspond to intervals 1.4, 1.5, 1.6, 1.7 in figure 5(*a*); spectra with flattening in the vicinity of the break correspond to intervals 1.8, 1.9, 1.10 in figure 5(*a*) and intervals 2.3, 2.4 in figure 5(*b*); spectra with a bump in the vicinity of the break correspond to intervals 2.5, 2.6, 2.7 in figure 5(*b*); spectra without steepening in the kinetic range correspond to intervals 2.8, 2.9 in figure 5(*b*). Thus the scaling can differ from one interval to another, but the clear deviation from the Kolmogorov scaling is observed for all intervals. The degree of distinction between the experimental scaling and the Kolmogorov model scaling can be different for the same type of spectra. For example type 1 spectra demonstrate weak deviation from the Kolmogorov scaling for the 1.2, 1.3 intervals of figure 5(*a*) and strong deviation for interval 1.1 in figure 5(*a*) and intervals 2.1, 2.3 in figure 5(*b*).

The experimental scaling in plasma turbulence can be well described and parameterized in the approach of She–Leveque–Dubrulle log-Poisson model (Budaev *et al.* 2011, 2015):

$$\zeta(q) = (1 - \Delta)\frac{q}{3} + \frac{\Delta}{1 - \beta_{SLD}}[1 - \beta_{SLD}^{q/3}], \tag{5.1}$$

https://doi.org/10.1017/S0022377817000502 Published online by Cambridge University Press

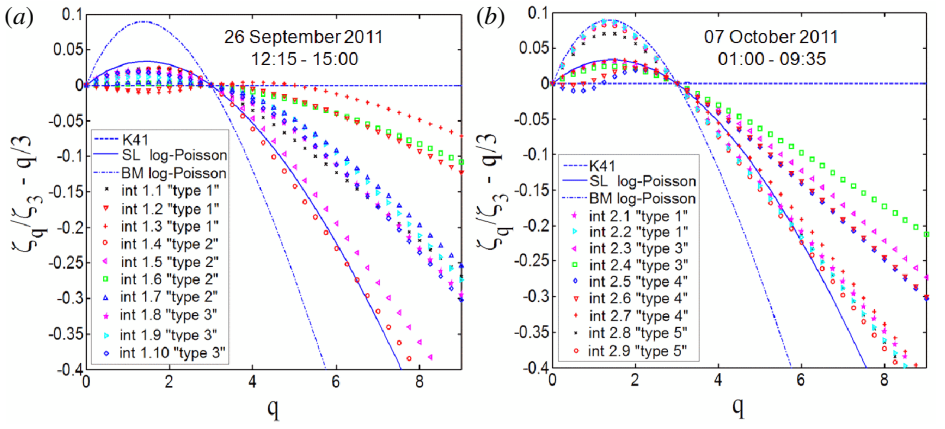

FIGURE 5. Comparison of the experimental scaling with the scaling of the Kolmogorov (K41) model (dashed line – $q/3$), the She–Leveque log-Poisson model (SL) (solid line) and with the Biskamp–Mueller (BM) log-Poisson model (dashed-dotted line). The curves of different colours and signs correspond to the scaling of the different selective subintervals with the different types of fluctuation spectra (the types are shown in the legend) on 26 September, 2011 12:15–15:00 UT (*a*) and on 7 October 2011 01:00–09:35 UT (*b*).

where Δ and β_{SLD} are changeable parameters, determined from analysis of experimental data. β_{SLD} determines the degree of intermittency: $\beta_{SLD} = 1$ for homogeneous developed turbulence without intermittency (as in the Kolmogorov model), $\beta_{SLD} < 1$ indicates an intermittent flow. The parameter Δ determines the scaling of energy $\varepsilon_l^\infty \sim l^{-\Delta}$ (l-scale parameter), where the energy rate value ε_l^∞ is limited by the presence of singular dissipative structures (Dubrulle 1994; She & Leveque 1994). Three-dimensional isotropic hydrodynamic turbulence is characterized by $\Delta = \beta_{SLD} = 2/3$ (She & Leveque 1994).

We calculate the parameterization coefficient for the data set used above. We determine the scaling $\zeta(q)$ by the Wavelet transform modulus maxima (WTMM) procedure (Budaev *et al.* 2011, 2015), based on wavelet analysis. This method takes into account the property of scale invariance of the turbulence and can significantly improve the accuracy of estimation of the high-order structure functions (up to $q = 9$ for the used number of points). We have found that the mean value of $\langle\beta_{SLD}\rangle = 0.1$ and $\langle\Delta\rangle = 0.2$, which proves the high level of intermittency for the majority of the analysed intervals. The value of Δ can be explained by the presence of dissipative structures with complicated fractal topology (Budaev *et al.* 2011, 2015). The $\beta_{SLD} \sim 1$ is observed only in 10 % of the events and can be associated with non-intermittent plasma flows for all kinds of fluctuation spectra. Riazantseva *et al.* (2015) have shown that the absence of intermittency is typically observed in the fast solar wind with a low density level but this statement cannot be reversed, high-velocity flow is not always characterized by a low level of intermittency. For example, spectra with nonlinear steepening in the kinetic range are generally characterized by high velocity (see § 4) but the majority of them are also characterized by a high level of intermittency.

The topology of dissipative structures affecting the scaling properties determines the selection of the model of three-dimensional isotropic turbulence. The two-dimensional

https://doi.org/10.1017/S0022377817000502 Published online by Cambridge University Press

current sheets are considered for the Biskamp–Mueller model (Biskamp & Mueller 2003), based on the traditional Iroshnikov–Kraichnan phenomenology for the plasma. The scaling can be written through the parameterization factor g as:

$$\zeta(q) = \frac{q}{g^2} + 1 - \left(\frac{1}{g}\right)^{q/g}. \tag{5.2}$$

On the other hand, one-dimensional filaments are considered for the She–Leveque model (She & Leveque 1994). Parameterization of the scaling in this case was proposed by Budaev (2009) and can be written through the parameterization factor g_f as:

$$\zeta_f(q) = \frac{q}{g_f^2} + 2\left(1 - \left(\frac{1+g_f}{2g_f}\right)^{q/g_f}\right). \tag{5.3}$$

The cascade efficiency in comparison to the Kolmogorov model is reflected in the values of coefficients g and g_f. A constant cascade of the energy rate is assumed in the anisotropic case and the scaling is supposed as $\delta_l \upsilon \sim l^{1/g}$ (where $\delta_l \upsilon$ is a velocity difference and l is a scale parameter, see Budaev *et al.* (2011)). The experimental scaling of the structure functions $\zeta(q)$ (reflected e.g. in figure 5) can be parameterized by g and g_f coefficients using the WTMM procedure (Budaev *et al.* 2011). Values of g or g_f of approximately 3 reflect the efficiency of the cascade and determines the choice of dominant contribution of the dissipation structures. Coefficient values higher or lower than 3 correspond to enhancement or depletion of the cascade, respectively. The mean values of geometrical parameterization parameters for all analysed intervals are equal to $\langle g \rangle = 2.5$ and $\langle g_f \rangle = 2.9$. Proximity of g_f value to 3 prefers a model with a dominant contribution of filament structures. The dominance of one-dimensional dissipation structures was also shown for the magnetic field fluctuations in the magnetospheric boundary layers (Budaev *et al.* 2011). Earlier Carbone *et al.* (1995) produced an analysis of high-order moments and compared the scaling laws between the low-frequency MHD turbulence in the solar wind, ordinary fluid flow and the She–Leveque model. The observed difference is explained by the contributions of different kinds of singular dissipative structures: two-dimensional planar sheets for the MHD solar wind turbulence and one-dimensional filaments for ordinary fluid flow. However, this analysis was produced only for the low-frequency solar wind turbulence whereas our analysis is concerned with the high-frequency solar wind plasma turbulence.

6. Discussion and conclusions

High time resolution plasma measurements allow us to focus on the features of the turbulence near the ion scales. The analysis of spectral and statistical properties of the high-frequency plasma fluctuations shows a non-stationary character of the turbulent flow. Various deviations of the frequency spectra and the probability distribution functions of fluctuations from the corresponding characteristics of classical stationary turbulence models can be observed.

It is known that the interplanetary magnetic field fluctuation spectra have different shapes in the fast and slow solar wind (Bruno & Carbone 2013). Whistler waves can lead to flattening in the high-frequency part of the magnetic field fluctuation spectra (Klein *et al.* 2014) and the Alfvén ion cyclotron waves can give rise to bumps in the spectra (Alexandrova 2008). The flattening at a frequency lower than

https://doi.org/10.1017/S0022377817000502 Published online by Cambridge University Press

the break frequency can be due to the contribution of coherent structures (Lion *et al.* 2016), kinetic Alfvén waves (e.g. Chandran *et al.* 2009) or thermal instabilities (e.g. Neugebauer *et al.* 1978). High variability of the magnetic field fluctuation spectra around the ion scales in the solar wind can be explained by the proportion of different physical processes which are working at these scales (Lion *et al.* 2016). The clear break is typical for a coherent spectrum whereas a spectrum with a smooth decrease without a break is observed for non-coherent fluctuations.

Several earlier density measurements exhibited predominately spectra with a flattening around the ion scales (Unti *et al.* 1973; Neugebauer *et al.* 1978; Celnikier *et al.* 1983; Kellogg & Horbury 2005; Chen *et al.* 2012) including recent Spektr-R measurements (Šafránková *et al.* 2013*a*,*b*, 2015) but the spectra of the ion flux fluctuations demonstrate predominately a shape with a clear break (Riazantseva *et al.* 2015). In this paper, we observe a wide variety of spectra in Spektr-R ion flux measurements and determine the relative proportion of different types of spectra. The most common shapes are spectra with two slopes and one break (∼50 %) and spectra with flattening in the vicinity of the break (∼32 %) often described in literature both for plasma and for the magnetic field fluctuations (see the review of Alexandrova *et al.* (2013)). Other shapes of spectra can be observed in a much smaller but not negligible number of cases: ∼6 % – spectra with nonlinear steepening in the kinetic range, ∼6 % – spectra without steepening in the kinetic range and ∼3 % – spectra with a bump in the vicinity of the break.

Using the joint analysis of Spektr-R and Wind measurements, we also determine typical plasma conditions for each type of spectra. The spectra with nonlinear steepening in the kinetic range are observed predominately for the solar wind with a rather high bulk velocity $V_p > 500$ km s^{-1}. This fact is consistent with the recently established relationship between bulk velocity and degree of spectra steepening for the magnetic field fluctuations (Bruno *et al.* 2014*a*,*b*). A significant part of the spectra with nonlinear steepening in the kinetic range is also connected with a high helium abundance and, to a lesser degree, by a large value of the density, the temperature, the magnetic field magnitude and the Alfvén velocity. The relationship between the turbulent properties and helium abundance seems to be a rather interesting point because the abundance of alpha particles can change the dispersive properties of the plasma and excite an instability which in turn can affect the spectrum of turbulent fluctuations (Hellinger & Travnicek 2013; Valentini 2016). The lowest values of plasma parameters are typical of spectra with a bump in the vicinity of the break and spectra without steepening in the kinetic range. Solar wind plasma parameters for spectra with two slopes and one break and spectra with a flattening in the vicinity of the break are rather ordinary. The peak of the distribution of Alfvén velocities for spectra with a bump in the vicinity of the break at low values is rather surprising but the statistics for this type of spectrum is poor. The role of the plasma parameter β_p is not clear from our statistics. We can say that low β_p is observed in approximately equal degrees for all types of spectra, whereas $\beta_p \sim 1$ and $\beta_p > 1$ can be observed predominately for spectra with two slopes and one break, spectra with nonlinear steepening in the kinetic range and spectra without a steepening in the kinetic range. The examples discussed in § 3 demonstrate the organization of the break frequency (where it can be determined) by β_p: the break tends to be controlled by the inertial length frequency for low β_p and by the gyrostructure frequency for high β_p, as it was earlier shown for the interplanetary magnetic field spectra (Chen *et al.* 2014*b*). The investigation of the relationship between spectrum shape and β_p should continue using a set containing extreme values of β_p.

https://doi.org/10.1017/S0022377817000502 Published online by Cambridge University Press

The probability distribution functions of the ion flux fluctuations and their statistical characteristics also vary considerably in the frequency range ~0.1–10 Hz for different intervals in the solar wind, but they always differ significantly from a Gaussian distribution. The increase of flatness (reflecting the deviation of distribution tails from the Gaussian distribution) at the high-frequency scales is observed for all shapes of fluctuation spectra in the solar wind and indicates the presence of intermittency. This was already shown for the magnetic field and plasma parameters in interplanetary medium up to the dissipation range (Bruno & Carbone 2013) but the plasma fluctuations in the kinetic range sometimes exhibit non-intermittent behaviour (Chen *et al.* 2014*a*).

The turbulence in all analysed intervals has a complicated multifractal structure and exhibits extended self-similarity which provide scale invariance to the system. This is true for the statistics presented in the paper and also for different turbulent plasma flows in space and the laboratory (Budaev *et al.* 2011, 2015). Herewith statistical and spectral properties of the ion flux fluctuations in the solar wind can be different for various plasma conditions. But this diversity lies inside the class of phenomena described in the sense of the ESS.

In a dominant part of the ion flux fluctuation measurements, the scaling of the structure functions may be well described by the log-Poisson model approach that takes into account the presence of intermittency. Using the log-Poisson parameterization we show the dominant contribution of filament-like structures in the formation of the solar wind plasma intermittency for intervals corresponding to different types of spectra in the solar wind. The geometry of the intermittent structures has been discussed for decades. The idea of the crucial role of filament structures in the solar wind ('spaghetti model') was born a long time ago on the basis of earlier solar wind observations (e.g. Bartley *et al.* 1966) and still remains relevant with the new experimental results (Bruno *et al.* 2001; Borovsky 2008). The authors have assumed that the solar wind consists of flow tubes of different sizes, with boundaries representing tangential discontinuities. They display the interlacement of tubes containing the distinct plasmas with different axial orientations for each. The intermittent events are located at the boundaries between of two adjacent flux tubes (Bruno *et al.* 2001). The possible relation of the dissipation mechanisms with the intermittent events (Matthaeus *et al.* 2015) has revived the interest in the topic of the geometry of the solar wind structures. A large number of authors have associated the intermittency in the solar wind turbulence with two-dimensional structures such as currents sheets (e.g. Boldyrev & Perez 2012; Greco *et al.* 2012; Perri *et al.* 2012). However, Alexandrova (2008) have shown that the intermittency in the solar wind turbulence is related to the filamentary structures such as Alfvén vortices. The analysis of high-order moments in Carbone *et al.* (1995) has shown that the most intermittent structures can be represented as filaments only for ordinary fluid flow, whereas for the low-frequency MHD solar wind turbulence they can be associated with the planar sheets. Budaev *et al.* (2011) have produced the log-Poisson parameterization of the high-order scaling for the turbulent space plasma in the boundary layers of the Earth's magnetosphere and demonstrated the better agreement with the model assuming one-dimensional dissipation structures. Later, it was proven for the solar wind plasma by using the high-resolution plasma measurements of Spektr-R (Budaev *et al.* 2015; Riazantseva *et al.* 2015). In this paper we also show the dominant role of the filamentary intermittent structures in the solar wind for a wide range of plasma parameters.

https://doi.org/10.1017/S0022377817000502 Published online by Cambridge University Press

Acknowledgements

The authors are grateful to all collaborators of the BMSW instrument both in Russia and in the Czech Republic. The data processing and analysis of Space Research Institute co-authors is supported by Russian Science Foundation project 16-12-10062, the Czech authors acknowledge support of the Czech Science Foundation via the project 16-04956S.

REFERENCES

ALEXANDROVA, O. 2008 Solar wind vs magnetosheath turbulence and Alfvén vortices. *Nonlinear Process. Geophys.* **15**, 95–108.

ALEXANDROVA, O., CARBONE, V., VELTRI, P. & SORRISO-VALVO, L. 2008 Small-scale energy cascade of the solar wind turbulence. *Astrophys. J.* **674**, 1153–1157.

ALEXANDROVA, O., CHEN, C. H. K., SORISSO-VALVO, L., HORBURY, T. S. & BALE, S. D. 2013 Solar wind turbulence and the role of ion instabilities. *Space Sci. Rev.* **178** (2–4), 101–139.

ALEXANDROVA, O., SAUR, J., LACOMBE, C., MANGENEY, A., MITCHELL, J., SCHARTZ, J. & ROBERT, P. 2009 Universality of solar-wind turbulent spectrum from MHD to electron scales. *Phys. Rev. Lett.* **103** (16), 165003.

BARTLEY, W. C., BAKATA, R. P., MCCRACKEN, K. G. & RAO, U. R. 1966 Anisotropic cosmic radiation fluxes of solar origin. *J. Geophys. Res.* **71** (13), 3297–3304.

BENZI, R., CILIBERTO, S., BAUDET, C., RUIZ CHAVARRIA, G. & TRIPICCIONE, R. 1993 Extended selfsimilarity in turbulent flows. *Phys. Rev.* E **48**, 29–35.

BISKAMP, D. 1994 Cascade models for magnetohydrodynamic turbulence. *Phys. Rev.* **50** (4), 2702–2711.

BISKAMP, D. & MUELLER, W. C. 2003 Statistical anisotropy of, magnetohydrodynamic turbulence. *Phys. Rev.* E **67**, 066302.

BOLDYREV, S. & PEREZ, J. C. 2012 Spectrum of kinetic-Alfvén turbulence. *Astrophys. J.* **758**, L44.

BOROVSKY, J. 2008 Flux tube texture of the solar wind: strands of the magnetic carpet at 1AU? *J. Geophys. Res.* **113**, A08110.

BOROVSKY, J. 2012 The velocity and magnetic field fluctuations of the solar wind at 1 AU: statistical analysis of Fourier spectra and correlations with plasma properties. *J. Geophys. Res.* **117**, A05104.

BOUROUAINE, S., ALEXANDROVA, O., MARSCH, E. & MAKSIMOVIC, M. 2012 On spectral breaks in the power spectra of magnetic fluctuations in fast solar wind between 0.3 and 0.9 AU. *Astrophys. J.* **749** (102), 7.

BRUNO, R. & CARBONE, V. 2013 The solar wind as a turbulence laboratory. *Liv. Rev. Sol. Phys.* **10** (1), 2, 208 pp.

BRUNO, R., CARBONE, V., SORRISO-VALVO, L. & BAVASSANO, B. 2003 Radial evolution of solar wind Intermittency in the inner heliosphere. *J. Geophys. Res.* **108**, 1130.

BRUNO, R., CARBONE, V., VELTRI, P., PIETROPAOLO, E. & BAVASSANO, B. 2001 Identifying intermittency events in the solar wind. *Planet. Space Sci.* **49** (12), 1201–1210.

BRUNO, R., TELLONI, D., PRIMAVERA, L., PIETROPAOLO, E., D'AMICISI, R., SORRISO-VALVO, L., CARBONE, V., MALARA, F. & VELTRI, P. 2014*b* Radial evolution of intermittency of density fluctuations in the fast solar wind. *Astrophys. J. Lett.* **786** (1), 53.

BRUNO, R., TRENCHI, L. & TELLONI, D. 2014*a* Spectral slope variation at proton scales from fast to slow solar wind. *Astrophys. J. Lett.* **793** (1), L15.

BUDAEV, V. P. 2009 Scaling properties of intermittent edge plasma turbulence. *Phys. Lett.* A **373**, 856–861.

BUDAEV, V. P., SAVIN, S. P. & ZELENYI, L. M. 2011 Investigation of intermittency and generalized self-similarity of turbulent boundary layers in laboratory and magnetospheric plasmas: towards a quantitative definition of plasma transport features. *Phys. Uspekhi* **54** (9), 875–918.

BUDAEV, V. P., ZELENYI, L. M. & SAVIN, S. P. 2015 Generalized self-similarity of intermittent plasma turbulence in space and laboratory plasmas. *J. Plasma Phys.* **81**, 395810602.

BURLAGA, L. F. 1991 Intermittent turbulence in the solar wind. *J. Geophys. Res.* **96** (A4), 5847–5851.

CARBONE, V., VELTRI, P. & BRUNO, R. 1995 Experimental evidence for differences in the extended self-similarity scaling laws between fluid and magnetohydrodynamic turbulent flows. *Phys. Rev. Lett.* **75** (17), 3110–3113.

CELNIKIER, L. M., HARVEY, C. C., JEGOU, R., MORICET, P. & KEMP, M. 1983 A determination of the electron density fluctuation spectrum in the solar wind, using the ISEE propagation experiment. *Astron. Astrophys.* **126** (2), 293–298.

CHANDRAN, B. D. G., QUATAERT, E., HOWES, G., XIA, Q. & PONGKITIWANICHAKUL, P. 2009 Constraining low-frequency Alfvénic turbulence in the solar wind using density fluctuations measurement. *Astrophys. J.* **707**, 1668.

CHEN, C. H. K., LEUNG, L., BOLDYREV, S., MARUCA, B. A. & BALE, S. D 2014*b* Ion-scale spectral break of solar wind turbulence at high and low beta. *Geophys. Res. Lett.* **41**, 8081–8088.

CHEN, C. H. K., SALEM, C. S., BONNELL, J. W., MOZER, F. S. & BALE, S. D. 2012 Density fluctuation spectrum on solar wind turbulence between ion and electron scales. *Phys. Rev. Lett.* **109**, 035001.

CHEN, C. H. K., SORRISO-VALVO, L., ŠAFRÁNKOVÁ, J. & NĚMEČEK, Z. 2014*a* Intermittency of solar wind density fluctuations from ion to electron scales. *Astrophys. J. Lett.* **789** (L8), 5.

DUBRULLE, B. 1994 Intermittency in fully developed turbulence: log-Poisson statistics and generalized scale covariance. *Phys. Rev. Lett.* **73**, 959.

DUDOK DE WIT, T., ALEXANDROVA, O., FURNO, I., SORRISO-VALVO, L. & ZIMBARDO, G. 2013 Methods for characterising microphysical processes in plasmas. *Space Sci. Rev.* **178** (2), 665–693.

FRISCH, U. 1995 *Turbulence*. Cambridge University Press.

GALTIER, S. 2006 Wave turbulence in incompressible Hall magnetohydrodynamics. *J. Plasma Phys.* **72**, 721–769.

GARY, P. S. 2015 Short-Wavelength turbulence and temperature anisotropy instabilities: recent computational progress (review). *Phil. Trans. R. Soc.* A **373**, 20140149.

GOLDSTEIN, M. L., ROBERTS, D. A. & MATTHAEUS, W. H. 1995 Magnetohydrodynamic turbulence in the solar wind. *Annu. Rev. Astron. Astrophys.* **33**, 283–325.

GOLDREICH, P. & SRIDHAR, S. 1995 Toward a theory of interstellar turbulence. II. Strong Alfvénic turbulence. *Astrophys. J.* **438** (2), 763–775.

GRAPPIN, R., VELLI, M. & MANGENEY, A. 1991 Alfvénic versus standard turbulence in the solar wind. *Ann. Geophys.* **9**, 416–426.

GRECO, A., MATTHAEUS, W. H., D'AMICIS, R., SERVIDIO, S. & DMITRUK, P. 2012 Evidence for nonlinear development of magnetohydrodynamic scale intermittency in the inner heliosphere. *Astrophys. J.* **749**, 105.

HELLINGER, P. & TRAVNICEK, P. M. 2013 Protons and alpha particles in the expanding solar wind: hybrid simulations. *J. Geophys. Res.* **118**, 5421–5430.

HNAT, B., CHAPMAN, S. C. & ROWLANDS, G. 2003 Intermittency, scaling, and the Fokker–Planck approach to fluctuations of the solar wind bulk plasma parameters as seen by the WIND spacecraft. *Phys. Rev.* E **67** (5), 056404.

HNAT, B., CHAPMAN, S. C. & ROWLANDS, G. 2005 Compressibility in solar wind plasma turbulence. *Phys. Rev. Lett.* **94** (20), 204502.

HORBURY, T. S., FORMAN, M. & OUGHTON, S. 2008 Anisotropic scaling of magnetohydrodynamic turbulence. *Phys. Rev. Lett.* **101**, 175005.

HOWES, G. G., COWLEY, S. C., DORLAND, V., HAMMETT, W., QUATAERT, E. & SCHEKOCHIHIN, A. A. 2008 A model of turbulence in magnetized plasmas: implications for the dissipation range in the solar wind. *J. Geophys. Res.* **113** (A12), 5103.

KELLOGG, P. J. & HORBURY, T. S. 2005 Rapid density fluctuations in the solar wind. *Ann. Geophys.* **23** (12), 3765–3773.

KIYANI, K. H., CHAPMAN, S. C., KHOTYAINTSEV, Y. V., DUNLOP, M. W. & SAHRAOUI, F. 2009 Global scale-invariant dissipation in collisionless plasma turbulence. *Phys. Rev. Let.* **103** (7), 075006.

KLEIN, K. G., HOWES, G. G. & TENBARGE, J. M. 2014 The violation of the Taylor hypothesis in measurements of solar wind turbulence. *Astrophys. J. Lett.* **790** (2), L20.

KOLMOGOROV, A. N. 1941 The local structure of turbulence in incompressible viscous fluid for very large Reynolds' numbers. *Dokl. Akad. Nauk. SSSR* **30** (4), 301–305.

LEAMON, R. J., SMITH, C. W., NESS, N. F., MATTHAEUS, W. H. & WONG, H. K. 1998 Observational constraints on the dynamics of the interplanetary magnetic field dissipation range. *J. Geophys. Res.* **103**, 4775–4787.

LION, S., ALEXANDROVA, O. & ZASLAVSKY, A. 2016 Coherent events and spectral shape at ion kinetic scales in the fast solar wind turbulence. *Astrophys. J.* **824** (1), 47, 13.

MARKOVSKII, S. A., VASQUEZ, B. J. & SMITH, C. W. 2008 Statistical analysis of the high-frequency spectral break of the solar wind turbulence at 1 AU. *Astrophys. J.* **675** (2), 1576–1583.

MARSCH, E. & TU, C.-Y. 1990 Spectral and spatial evolution of compressible turbulence in the inner solar wind. *J. Geophys. Res.* **95** (8), 11945–11956.

MARSCH, E. & TU, C. Y. 1997 Intermittency, non-Gaussian statistics and fractal scaling of MHD fluctuations in the solar wind. *Nonlinear Process. Geophys.* **4** (2), 101–124.

MATTHAEUS, W. H. & VELLI, M. 2011 Who needs turbulence? *Space Sci. Rev.* **160**, 145.

MATTHAEUS, W. H., WAN, M., SERVIDIO, S., GRECO, A., OSMAN, K. T., OUGHTON, S. & DMITRUK, P. 2015 Intermittency, nonlinear dynamics and dissipation in the solar wind and astrophysical plasmas. *Phil. Trans. R. Soc.* A **373**, 20140154.

NEUGEBAUER, M., WU, C. S. & HUBA, J. D. 1978 Plasma fluctuations in the solar wind. *J. Geophys. Res.* **83** (3), 1027–1034.

NOVIKOV, E. A. & STEWART, R. 1964 Intermittency of turbulence and spectrum of fluctuations in energy-dissipation. *Izv. Akad. Nauk. SSSR Ser. Geofiz.* **3**, 408–412.

PERRI, S., CARBONE, V. & VELTRI, P. 2010 Where does fluid-like turbulence break down in the solar wind. *Astrophys. J. Lett.* **725**, L52–L55.

PERRI, S., GOLDSTEIN, M. L., DORELLI, J. C. & SAHRAOUI, F. 2012 Detection of small-scale structures in the dissipation regime of solar-wind turbulence. *Phys. Rev. Lett.* **109**, 191101.

PITŇA, A., ŠAFRÁNKOVÁ, J., NĚMEČEK, Z., GONCHAROV, O., NĚMEC, F., PŘECH, L., CHEN, C. H. K. & ZASTENKER, G. N. 2016 Density fluctuations upstream and downstream of interplanetary shocks. *Astrophys. J.* **819** (1), 41, 9.

PODESTA, J. J. 2013 Evidence of kinetic Alfvén waves in the solarwind at 1 AU. *Solar Phys.* **286**, 529–548.

PODESTA, J. J., ROBERTS, D. A. & GOLDSTEIN, M. L. 2006 Power spectrum of small-scale turbulent velocity fluctuations in the solar wind. *J. Geophys. Res.* **111**, A10109.

RAKHMANOVA, L., RIAZANTSEVA, M. & ZASTENKER, G. 2016 Plasma fluctuations at the flanks of the Earth's magnetosheath at ion kinetic scales. *Ann. Geophys.* **34**, 1011–1018.

RAKHMANOVA, L. S., RIAZANTSEVA, M. O., ZASTENKER, G. N. & YERMOLAEV, YU. 2017 High frequency plasma fluctuations in the middle magnetosheath and near its boundaries: spectr-R observations. *J. Plasma Phys.* **83**, 705830204.

RIAZANTSEVA, M. O., BUDAEV, V. P., RAKHMANOVA, L. S., ZASTENKER, G., SAFRANKOVA, J., NEMECEK, Z. & PRECH, L. 2016 Comparison of properties of small-scale ion flux fluctuations in the flank magnetosheath and in the solar wind. *Adv. Space Res.* **58** (2), 166–174.

RIAZANTSEVA, M. O., BUDAEV, V. P., ZELENYI, L. M., ZASTENKER, G., PAVLOS, G. P., SAFRANKOVA, J., NEMECEK, Z., PRECH, L. & NEMEC, F. 2015 Dynamic properties of small scale solar wind plasma fluctuations. *Phil. Trans. R. Soc.* A **373**, 20140146.

RIAZANTSEVA, M. O. & ZASTENKER, G. N. 2008 The intermittency of ion density fluctuations and it's relation with sharp density changings. *Cosmic Res.* **46** (1), 3–9.

RIAZANTSEVA, M. O., ZASTENKER, G. N. & KARAVAEV, M. V. 2010 Intermittency of solar wind ion flux and magnetic field fluctuations in the wide frequency region from 10^{-5} up to 1 Hz and the influence of sudden changes of ion flux. In *Solar Wind 12 Proceedings, AIP Conference Proceedings*, vol. 1216, (1), pp. 132–135. AIP.

ROBERTS, O. W., LI, X., ALEXANDROVA, O. & LI, B. 2016 Observation of an MHD Alfvén vortex in the slow solar wind. *J. Geophys. Res.* **121** (5), 3870–3881.

ŠAFRÁNKOVÁ, J., NĚMEČEK, Z., PŘECH, L., ZASTENKER, G., ČERMÁK, I., CHESALIN, L., KOMÁREK, A., VAVERKA, J., BERÁNEK, M., PAVLŮ, J. *et al.* 2013*a* Fast solar wind monitor (BMSW): description and first results. *Space Sci. Rev.* **175** (1–4), 165–182.

ŠAFRÁNKOVÁ, J., NĚMEČEK, Z., NEMEC, F., PITNA, A., CHEN, C. H. K. & ZASTENKER, G. 2015 Solar wind density spectra around the ion spectral break. *Astrophys. J.* **803** (2), 107, 7.

ŠAFRÁNKOVÁ, J., NĚMEČEK, Z., NĚMEC, F., PŘECH, L., CHEN, C. H. K. & ZASTENKER, G. N. 2016 Power spectral density of fluctuations of bulk and thermal speeds in the solar wind. *Astrophys. J.* **825** (2), 121, 8.

ŠAFRÁNKOVÁ, J., NĚMEČEK, Z., PŘECH, L. & ZASTENKER, G. 2013*b* Ion kinetic scale in the solar wind observed. *Phys. Rev. Lett.* **110**, 025004.

SAHRAOUI, F., GOLDSTEIN, M. L., ROBERT, P. & KHOTYAINTSEV, Y. V. 2009 Evidence of a cascade and dissipation of solar-wind turbulence at the electron gyroscale. *Phys. Rev. Lett.* **102**, 231102.

SALEM, C., MANGENEY, A., BALE, S. & VELTRI, P. 2009 Solar wind magnetohydrodynamics turbulence: anomalous scaling and role of intermittency. *Astrophys. J.* **702** (1), 537–553.

SCHEKOCHIHIN, A. A., COWLEY, S. C., DORLAND, W., HAMMETT, W., HOWES, G., QUATAERT, E. & TATSUNO, T. 2009 Astrophysical gyrokinetics: kinetic and fluid turbulent cascades in magnetized weakly collisional plasmas. *Astrophys. J. Suppl. Ser.* **182**, 310–377.

SERVIDIO, S., CARBONE, V., PRIMAVERA, L., VELTRI, P. & STASIEWICZ, K. 2007 Compressible turbulence in Hall magnetohydrodynamics. *Planet. Space Sci.* **55**, 2239–2243.

SERVIDIO, S., VALENTINI, F., PERRONE, D., GRECO, A., CALIFANO, F., MATTHAEUS, W. H. & VELTRI, P. 2015 A kinetic model of plasma turbulence. *J. Plasma Phys.* **81**, 325810107.

SHE, Z. S. & LEVEQUE, E. 1994 Universal scaling laws in fully developped turbulence. *Phys. Rev. Lett.* **72** (3), 336–339.

SMITH, C. W., HAMILTON, K., VASQUEZ, B. J. & LEAMON, R. J. 2006 Dependence of the dissipation range spectrum of interplanetary magnetic fluctuations on the rate of energy cascade. *Astrophys. J.* **645**, 85–88.

SORRISO-VALVO, L., CARBONE, V., VELTRI, P., CONSOLINI, G. & BRUNO, R. 1999 Intermittency in the solar wind turbulence through probability distribution functions of fluctuations. *Geophys. Res. Lett.* **26**, 1801–1804.

UNTI, T. W. J., NEUGEBAUER, M. & GOLDSTEIN, B. E. 1973 Direct measurements of solar-wind fluctuations between 0.0048 and 13.3 Hz. *Astrophys. J.* **180**, 591–598.

VAIVADS, A. *et al.* 2016 Turbulence Heating ObserveR – satellite mission proposal. *J. Plasma Phys.* **82**, 905820501.

VALENTINI, F. *et al.* 2016 Differential kinetic dynamics and heating of ions in the turbulent solar wind. *N. J. Phys.* **18** (12), 125001.

ZASTENKER, G. N. *et al.* 2013 Fast measurements of solar wind parameters by BMSW instrument. *Cosmic Res.* **51** (2), 78–89.

ZELENYI, L. M. & MILOVANOV, A. V. 2004 Fractal topology and strange kinetics: from percolation theory to problems in cosmic electrodynamics. *Phys.-Usp.* **47** (8), 749.

YERMOLAEV, Y. I., NIKOLAEVA, N. S., LODKINA, I. G. & YERMOLAEV, M. Y. 2009 Catalog of large-scale solar wind phenomena during 1976–2000. *Cosmic Res.* **47** (2), 81–94.

YORDANOVA, E., BALOGH, A., NOULLEZ, A. & VON STEIGER, R. 2009 Turbulence and intermittency in the heliospheric magnetic field in fast and slow solar wind. *J. Geophys. Res.* **114**, A08101.